Systematic design and fabrication of high-Q single-mode pulley-coupled planar silicon nitride microdisk resonators at visible wavelengths

Ehsan Shah Hosseini, Siva Yegnanarayanan, Amir Hossein Atabaki , Mohammad Soltani, and Ali Adibi*

School of Electrical and Computer Engineering, Georgia Institute of Technology, 777 Atlantic Drive NW, Atlanta, GA 30332–0250, U.S.A.

**adibi@ece.gatech.edu*

Abstract: High quality ($Q \approx 6 \times 10^5$) microdisk resonators are demonstrated in a Si_3N_4 on SiO_2 platform at 652–660 nm with integrated in-plane wrap-around coupling waveguides to enable critical coupling to specific microdisk radial modes. Selective coupling to the first three radial modes with >20dB suppression of the other radial modes is achieved by controlling the wrap-around waveguide width. Advantages of such pulley-coupled microdisk resonators include single mode operation, ease of fabrication due to larger waveguide-resonator gaps, the possibility of resist reflow during the lithography phase to improve microdisk etched surface quality, and the ability to realize highly over-coupled microdisks suitable for low-loss delay lines and add-drop filters.

OCIS codes: (130.3120) Integrated optics devices; (230.5750) Resonators.

References and links

1. S. Blair and Y. Chen, "Resonant-enhanced evanescent-wave fluorescence biosensing with cylindrical optical cavities." Appl. Opt. **40**, 570–582 (2001).
2. A. Armani, R. Kulkarni, S. Fraser, R. Flagan, and K. Vahala, "Label-free, single-molecule detection with optical microcavities," Science **317**, 783–787 (2007).
3. F. Vollmer and S. Arnold, "Whispering-gallery-mode biosensing: label-free detection down to single molecules," Nat. Methods **5**, 591–596 (2008).
4. T. Barwicz, M. Popović, P. Rakich, M. Watts, H. Haus, E. Ippen, and H. Smith, "Microring-resonator-based add-drop filters in SiN: fabrication and analysis." Opt. Express **12**, 1437–1442 (2004).
5. J. Hryniewicz, P. Absil, B. Little, R. Wilson, and P. Ho, "Higher order filter response in coupled microring resonators," IEEE Photon. Technol. Lett. **12**, 320–322 (2000).
6. P. Barclay, K. Srinivasan, O. Painter, B. Lev, and H. Mabuchi, "Integration of fiber-coupled high-Q SiN microdisks with atom chips," Appl. Phys. Lett. **89**, 131108 (2006).
7. M. Soltani, S. Yegnanarayanan, and A. Adibi, "Ultra-high Q planar silicon microdisk resonators for chip-scale silicon photonics." Opt. Express **15**, 4694–4704 (2007).
8. D. Jeanmaire and R. Van Duyne, "Surface Raman spectroelectrochemistry. Part I. Heterocyclic, aromatic, and aliphatic amines adsorbed on the anodized silver electrode," J. Electroanal. Chem. **84**, 1–20 (1977).
9. E. C. Le Ru and P. Etchegoin, *Principles of Surface-Enhanced Raman Spectroscopy: And Related Plasmonic Effects* (Elsevier, 2008).
10. E. Krioukov, D. Klunder, A. Driessen, J. Greve, and C. Otto, "Two-photon fluorescence excitation using an integrated optical microcavity: a promising tool for biosensing of natural chromophores," Talanta **65**, 1086–1090 (2005).

#119623 - $15.00 USD Received 6 Nov 2009; revised 15 Jan 2010; accepted 15 Jan 2010; published 19 Jan 2010

11. E. Shah Hosseini, S. Yegnanarayanan, A. H. Atabaki, M. Soltani, and A. Adibi, "High quality planar silicon nitride microdisk resonators for integrated photonics in the visible wavelength range," Opt. Express **17**, 14543–14551 (2009).
12. A. Yariv, "Universal relations for coupling of optical power between microresonators and dielectric waveguides," Electron. Lett. **36**, 321–322 (2000).
13. M. Chin and S. Ho, "Design and Modeling of Waveguide-Coupled Single-Mode Microring Resonators," J. Lightwave Technol. **16**, 1433–1446 (1998).
14. J. Hu, N. Carlie, N. Feng, L. Petit, A. Agarwal, K. Richardson, and L. Kimerling, "Planar waveguide-coupled, high-index-contrast, high-Q resonators in chalcogenide glass for sensing," Opt. Lett. **33**, 2500–2502 (2008).
15. S. Chuang, "A coupled mode formulation by reciprocity and a variational principle," J. Lightwave Technol. **5**, 5–15 (1987).
16. M. Born and E. Wolf, *Principles of optics: electromagnetic theory of propagation, interference and diffraction of light* (Cambridge University Press, 1999).
17. C. Manolatou, M. Khan, S. Fan, P. Villeneuve, H. Haus, and J. Joannopoulos, "Coupling of modes analysis of resonant channel add-drop filters," IEEE J. Quantum Electron. **35**, 1322–1331 (1999).
18. M. Soltani, "Novel integrated silicon nanophotonic structures using ultra-high *Q* resonators," Ph.D. thesis, Georgia Institute of Technology (2009).

1. Introduction

High quality traveling-wave optical resonators have recently attracted significant attention for several applications including sensing, nonlinear optics, and quantum optics [1–3]. One important requirement for such applications is strong light-matter interaction, which is enabled by high quality factor (Q) of the resonator modes. Another desired feature is the possibility of single mode operation (i.e., coupling to only one radial mode of the resonator). In addition, full control over the coupling of the resonators to the adjacent waveguides on the same substrate enables the design and implementation of a variety of devices. The three resonance structures commonly used in integrated planar implementations are microrings [4], racetracks [5], and microdisks [6, 7], among which microdisk resonators demonstrate higher quality factors due to less scattering because of only one etched sidewall [7].

Realization of whispering gallery mode (WGM) resonators in silicon-based material systems has great benefits, such as ease of fabrication, integrability with mature silicon (Si) electronics, and low cost. Unfortunately, silicon is very lossy in the visible and near infrared (NIR) wavelengths, which are more appropriate for most biological sensing applications such as fluorescence sensing [1] and surface enhanced Raman spectroscopy (SERS) [8, 9]. On the other hand, silicon nitride (Si_3N_4) with its low loss and fairly high refractive index ($n \approx 2$) in the visible and NIR range offers an inexpensive and Si-compatible platform for visible sensing applications. Thus, provided that the Si_3N_4 layer is optically isolated from the lossy Si substrate, it can guide the visible light without significant loss in this wavelength range. Krioukov et al. reported a microring-based Si_3N_4 sensor in the visible range using a resonator with a moderate quality factor ($Q \approx 1600$) [10]. Barclay et al. demonstrated a very high Q undercut Si_3N_4 microdisk resonator in the NIR, but the bulky tapered fiber coupling scheme makes such structures difficult to use in compact, integrated biosensors.

Recently, we demonstrated high Q, planar Si_3N_4 microdisk resonators in the visible range, in which coupling to the resonator is achieved by an optical waveguide (WG) side-coupled to the resonator [11]. When the waveguide is side-coupled to the resonator at a single point, the critical coupling condition [12] requires a very narrow coupling gap (gap < 100 nm) between the waveguide and the resonator. In order to ease the fabrication, we have proposed a rib-like configuration in which a thin layer of the guiding material (Si_3N_4) (that is achieved by partial plasma dry etching) increases the field overlap between the coupled elements thus increasing the coupling coefficient [11]. Nevertheless, such rib-type structures require an accurate control over the etch depth to achieve the targeted "pedestal" height. In addition, single-mode operation is hard to achieve in such rib-type structures. Another effective, yet seldom investigated,

#119623 - $15.00 USD Received 6 Nov 2009; revised 15 Jan 2010; accepted 15 Jan 2010; published 19 Jan 2010

approach to increase the gap size and thus ease the fabrication is increasing the effective coupling length rather than the field overlap. In this approach, termed "pulley" coupling, the waveguide wraps around the resonator (e.g., a microdisk), effectively increasing the coupling length several times compared to the single point coupling with a straight waveguide. This approach was initially modeled with conformal transformation method [13] and recently utilized in a chalcogenide glass sensor. [14]. However, a thorough investigation of this technique is needed to develop a systematic design approach for high Q resonators with whispering gallery modes.

In this work, a systematic analysis of pulley-coupled, high Q, Si_3N_4/SiO_2 resonators is presented. We also demonstrate the coupling of the resonators to wrap-around waveguides in the visible wavelength range (at λ=652-660 nm). We will show that not only are wider coupling gaps possible using the pulley coupling scheme, but also the strict phase matching condition makes the coupling single mode. Therefore, with the proper choice of the wrap-around waveguide width, only one of the radial modes of the microdisk is excited while the other radial modes are uncoupled from the waveguide field. These advantages (single mode operation, critical coupling with easy-to-fabricate gap size, and high Q) make the resonance structures presented here an excellent choice for applications that require strong light matter interaction.

2. Fabrication

A scanning electron micrograph (SEM) of a typical pulley-coupled microdisk resonator discussed in this paper is shown in Fig. 1(a). The SEM of a similar microdisk resonator with a single-point coupling to a waveguide is shown in Fig. 1(b) for comparison. Fabrication of these structures is done on top of a 6-micron-thick oxide layer, which isolates the guiding Si_3N_4 layer from the lossy Si substrate (see [11] for more detail). A 200 ± 3 nm-thick layer of low loss, stoichiometric Si_3N_4 is then deposited on top of the oxide using low pressure chemical vapor deposition (LPCVD). 500 nm of ZEP-520 electron beam resist is used as the etching mask and the structures are patterned using a JEOL JBX-9300FS 100kV electron beam lithography system. It has been shown that reflowing the resist after development leads to smoother sidewalls resulting in higher Q's [6]. Therefore, the developed patterns on ZEP are reflowed on a hot plate at 160°C for 3–5 minutes depending on the desired sidewall smoothness and sidewall angle. Longer reflow times results in smoother sidewalls (as can be seen in Fig. 1(c) for a 5 minute reflow) but requires wider gap sizes as a longer reflow leads to more tilted sidewalls and the bottom of the waveguide and resonator patterns on ZEP stick to each other during the reflow process (the rest of the paper is based on the 3 minute reflow). With the 3 minute reflow process performed within 24 hours from the resist spinning, the waveguides become 90 ± 10 nm narrower than the e-beam written patterns (measured at the middle of the waveguide). Etching is then performed using CF_4 gas in an inductively coupled plasma (ICP) etcher. The sidewall roughness is inspected with scanning electron microscopy which shows very high quality of the sidewalls.

3. Characterization and Discussion

To characterize the fabricated structures, the output light of a tunable laser diode source is coupled to the cleaved facet of the waveguide using a microscope objective lens. The wavelength of the laser is swept across the 652–660 nm wavelength range in 0.25 pm steps, and the transmission is measured as a function of wavelength by a Si detector at the waveguide output. The polarization of interest in this work is quasi-TE (quasi-transverse electric) i.e., the mode for which the electric field is mainly in the plane of the resonator. (For the sake of brevity, we call quasi-TE and quasi-TM (quasi-transverse magnetic) modes simply TE and TM

#119623 - $15.00 USD Received 6 Nov 2009; revised 15 Jan 2010; accepted 15 Jan 2010; published 19 Jan 2010

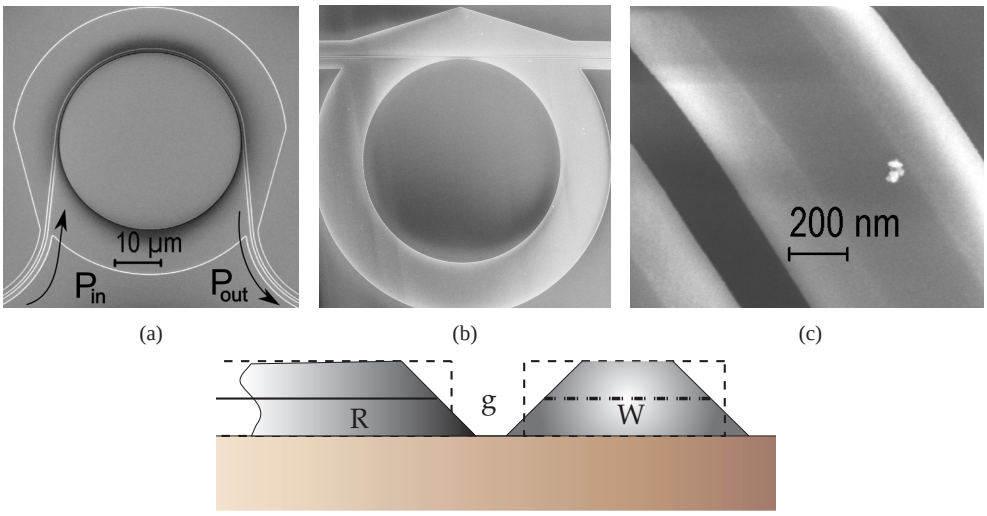

Fig. 1. (a) The pulley coupling configuration in which the waveguide wraps around the microdisk resonator to increase the effective coupling length. The phase matching to different radial modes of the microdisk is achieved by the choice of the waveguide width. (b) The conventional straight coupling configuration in which the waveguide couples to the microdisk only at a single point. In this configuration the effective interaction length is significantly shorter than the pulley scheme depicted in (a), making the coupling much less sensitive to the phase matching condition. (c) Top view of an SEM image of a waveguide etched on a 200 nm layer of Si_3N_4 on top of an isolating SiO_2 layer on a Si substrate with a 5 minute reflow of the resist. The reflow process leads to smooth but tilted sidewalls. (d) The diagram showing the effect of the reflow process on the waveguide and the microdisk sidewalls.

throughout this paper. Figure 6 shows the transmission spectrum for such structures with the pulley configuration shown in Fig. 1(a). Each dip in Fig. 6 corresponds to a TE cavity mode.

The power transmission coefficient at the resonance frequency (ω_o) for the coupled structure in Fig. 1(a) is given by $T(\omega_o) = \left[(Q_o - Q_c)/(Q_o + Q_c)\right]^2$, where Q_o and Q_c are respectively the intrinsic Q and the coupling Q [12]. When $Q_o = Q_c$, the transmission coefficient of the waveguide becomes zero at the resonance frequency and the waveguide mode energy is completely transferred to the microresonator. This special situation, called critical coupling [12], can be achieved by optimizing the gap size, the phase matching condition, and the coupling length. We perform this optimization by detailed analysis of the structure in Fig. 1(a) for different waveguide-cavity gaps and waveguide sizes using the coupled-mode theory [15]. The microdisk and the waveguide are modeled in the COMSOL® finite element method (FEM) package [7]. To accurately model the resonator in Fig. 1(a), the index of the Si_3N_4 film is measured using ellipsometry and fitted to a Cauchy model [16]. The resulting value is $n \approx 2.07$ at 655 nm.

Our calculations show that to get significant coupling to the first few modes of a 20 μm radius disk with $Q < 1 \times 10^6$, the coupling gap should be narrower than 100 nm if the conventional single-point coupling to a straight waveguide [in Fig. 1(b)] is used. This is primarily due to the short effective interaction length in the single point side-coupling scheme in which the effective distance between the waveguide and the microdisk increases very rapidly as the wave travels along the waveguide. To address this issue, one can wrap the waveguide around the disk

#119623 - $15.00 USD Received 6 Nov 2009; revised 15 Jan 2010; accepted 15 Jan 2010; published 19 Jan 2010

to increase the effective interaction length from a few microns to ultimately 120 μm for 20 μm-radius disks (Fig. 2). Nevertheless, such a configuration requires a strict phase matching condition as unless the two traveling waves have the same phase velocity, the phase walk-off between them makes the coupling coefficient practically negligible. The power transmission coefficient of a straight waveguide and a wrap-around waveguide side-coupled to a microdisk is compared in Fig. 3(a) and Fig. 3(b).

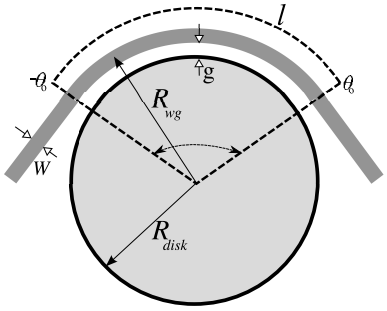

Fig. 2. The pulley coupling configuration in which the waveguide effectively interacts with the microdisk in the radial region between $-\theta_o$ and θ_o. R_{disk} is the radius of the disk (20 μm in this case), g is the coupling gap between the microdisk and the waveguide, W is the width of the waveguide, and $R_{wg}=R_{disk}+g+W/2$ is the effective radius of the curved waveguide.

To model this numerically, the coupling coefficient between a waveguide and an adjacent cavity is given by the first order temporal perturbation theory [15, 17, 18] as

$$\kappa = \int_{-\theta_o}^{\theta_o} \left[\frac{i\omega}{4} \int_0^W \int_0^d \left(\varepsilon(r,z)-\varepsilon_o\right)\right) \mathbf{E}_{\text{disk}} \cdot \mathbf{E}_{\text{wg}}\ r\,\mathrm{d}r\,\mathrm{d}z \right] e^{j\phi}\mathrm{d}\theta, \tag{1}$$

in which $\mathbf{E}_{\text{disk}}$ and $\mathbf{E}_{\text{wg}}$ correspond to the normalized amplitudes of the electric fields of the disk and the waveguide, respectively, θ_o is the angular range of the wrap-around coupling, d is the thickness of the guiding layer (i.e., Si_3N_4), and W is the width of the waveguide. $\varepsilon(r,z)-\varepsilon_o$ is the perturbation introduced to the microdisk mode by the waveguide and depends on the shape of the waveguide. Figure 2 shows the geometry of the coupled structures and the parameters used in our modeling. The phase factor ϕ in Eq. (1) is the difference between the propagation phases of the waveguide and the cavity modes and can be written as

$$\phi = -m\theta + \beta_{wg} R_{wg}\,\theta = -m\theta + k_o\, n_{wg} R_{wg}\,\theta, \tag{2}$$

in which $k_o = 2\pi/\lambda_o$ is the wavenumber in the free space, β_{wg} is the propagation constant of the waveguide mode, and m is the azimuthal mode order of the resonator. Apparently, the effective radius of the curved waveguide (R_{wg}) is larger than the radius of the disk ($R_{wg} = R_{disk}+g+W/2$). Assuming that the width of the waveguide (W) and the coupling gap (g) remain constant throughout the coupling length, the term inside the brackets in Eq. (1) is independent of θ and can be written as S, and κ from Eq. (1) can be simplified as

$$\kappa = S\int_{-\theta_o}^{\theta_o} e^{j\theta(k_o n_{wg} R_{wg} - m)}\mathrm{d}\theta = 2\theta_o S\,\mathrm{sinc}\left[(k_o n_{wg} R_{wg} - m)\frac{\theta_o}{\pi}\right], \tag{3}$$

where $\mathrm{sinc}(u) = \sin(\pi u)/(\pi u)$.

It is clear form Eq. (3) that the phase mismatch $(\theta_o\,(k_o n_{wg} R_{wg} - m))$ between the two structures can reduce the coupling coefficient considerably. If the phase matching condition

#119623 - $15.00 USD Received 6 Nov 2009; revised 15 Jan 2010; accepted 15 Jan 2010; published 19 Jan 2010

is met (i.e., $k_o n_{wg} R_{wg} = m$), the coupling coefficient is a linear function of the coupling length (which is proportional to θ_o). Conversely, if the phase mismatch builds up to a multiple of π, the coupling vanishes no matter how strong the field overlap is. It is also noteworthy that—similar to the results from the conformal transformation method for modeling waveguide-microring coupling [13]—the phase matching condition depends on the effective radius of the waveguide (R_{wg} in Fig. 2).

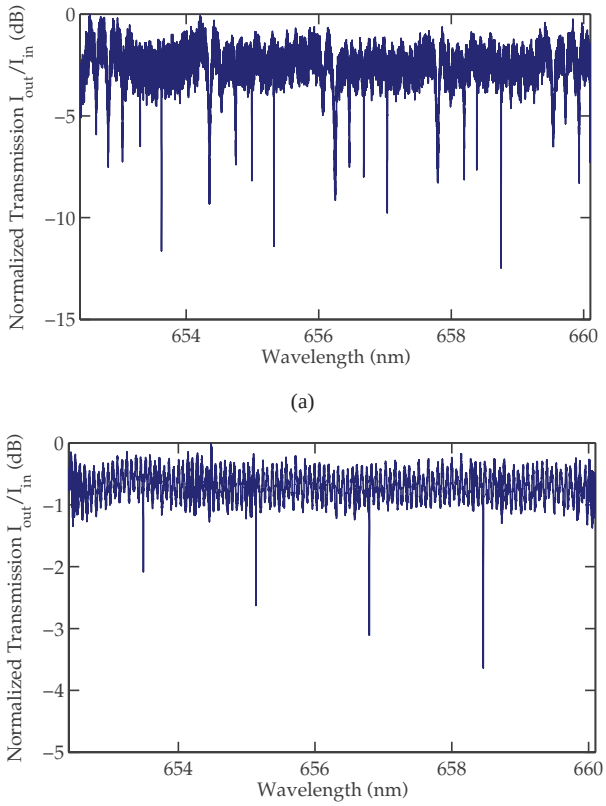

Fig. 3. (a) The normalized transmission spectrum of a 20-micron-radius Si_3N_4 microdisk side coupled to a waveguide with a single point coupling scheme [see Fig. 1(b)]. The coupling gap is 100 nm and several radial TE modes of the microdisk are excited. The waveguide width is 400 nm. The effective coupling length is about 4 μm. The polarization of the input waveguide is TE. (b) The normalized transmission of the waveguides coupled to the same microdisk as in (a) in the pulley configuration shown in Fig. 1(a). The coupling length is 30 μm and the coupling gap is 400 nm. The waveguide width is 390 nm and only the second radial order mode of the disk is excited. The strict phase matching condition does not allow the other radial modes of the microdisk to have significant coupling to the waveguide.

Since the phase velocity of different WGMs of the resonator in Fig. 2 vary across different radial modes, one can expect the phase matching condition to be mode-dependent. If the effective index of each radial mode is defined as ($n_{disk} \equiv m/k_o R_{disk}$), it is clear that the phase matching is achieved when $n_{wg} R_{wg} = n_{disk} R_{disk}$. The effective index of the waveguide is controllable by changing the waveguide width (W) within the range 150 nm $< W <$ 550

#119623 - $15.00 USD Received 6 Nov 2009; revised 15 Jan 2010; accepted 15 Jan 2010; published 19 Jan 2010

nm to ensure single mode guiding [11]. Increasing W results in larger effective indices for all waveguide modes. On the other hand, the effective indices of of different radial mode orders of the microdisk resonator depend on the geometrical properties of the microdisk. Noting that the lower order modes of the microdisk have higher effective indices, the required W for phase matching is the largest for the fundamental microdisk mode.

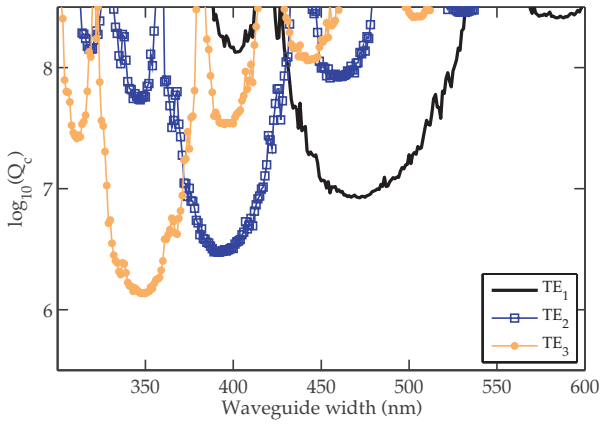

(a) $g = 400$ nm

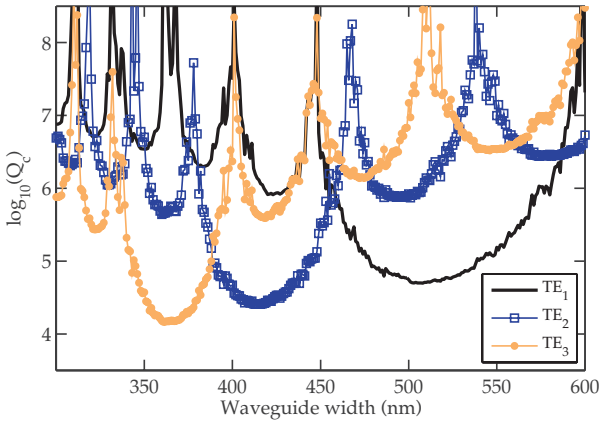

(b) $g = 200$ nm

Fig. 4. (a) The simulated coupling quality factor (Q_c) of a 20 μm radius disk at $\lambda = 650$ nm when the waveguide wraps around the disk and the coupling length is 30 μm. As the width of the waveguide is changed, the phase matching condition is met for three different radial order TE modes of the disk. (a) The coupling gap size is $g = 400$ nm and the phase matching condition is met for the first three orders of the disk when the waveguide width is 470, 390 and 340 nm respectively. (b) The gap size is reduced to $g = 200$ nm, without changing any other parameter compared to part (a). The coupling is enhanced almost two orders of magnitude for all three modes. As the phase matching condition depends on the radius of the curved waveguide, all microdisk modes are coupled to slightly wider waveguides.

We performed FEM simulations to obtain the field distribution of the first three radial microdisk TE modes (TE_1–TE_3) and the TE waveguide mode. We then use these field distributions (obtained from the COMSOL FEM simulations) in Eq. (1) to calculate the coupling coefficient (κ) between the cavity and the waveguide in the structure shown in Fig.

#119623 - $15.00 USD Received 6 Nov 2009; revised 15 Jan 2010; accepted 15 Jan 2010; published 19 Jan 2010

2. The calculated Q_c for the first three radial TE modes (TE_1–TE_3) as a function of W for waveguide-cavity gaps of $g = 400$ nm and $g = 200$ nm (see Fig. 2) is shown in Figs. 4(a) and 4(b), respectively. The coupling length for both cases is 30 μm The calculated κ is then used to find the coupling quality factor ($Q_c = \omega_o/\kappa^2$) as a function of the waveguide width for the waveguide-cavity coupled structure shown in Fig. 2. The minimum of each Q_c curve in Fig. 4 corresponds to the highest level of coupling between the waveguide and each corresponding cavity mode. As expected from Eq. (3), the optimal waveguide width for coupling to each cavity mode is slightly smaller at a larger gap size. Moreover, increasing the coupling length (l), while increasing the coupling coefficient (i.e. $\kappa \propto l$), reduces the reproducibly of the design as the tolerance to fabrication errors in the width of the fabricated waveguide is reduced almost linearly with l. It is important to note that with our current results for the intrinsic Q [e.g., $Q_o(TE_2) = 6 \times 10^5$ as shown in Fig. 3(b)] it is possible to achieve close to critical coupling (i.e., $Q_c = Q_o$) with gaps larger than 400 nm by using appropriate coupling length l. Figure 4(a) shows that with gaps as large as $g = 400$ nm, it is possible to achieve coupling Qs close to 10^6 for some modes ($Q_c = 1.37 \times 10^6$ for TE_3 and $Q_c = 3.0 \times 10^6$ for TE_2). We can further reduce Q_c (i.e., stronger coupling or larger κ) for the same gap size by increasing the coupling length. This considerably facilitates the fabrication process as explained earlier. It is also clear from Fig. 4(a) that at the optimal coupling width (W) for each TE mode, coupling to the other modes is negligible due to the phase mismatch. This facilitates the highly desired single mode operation of the high Q resonators.

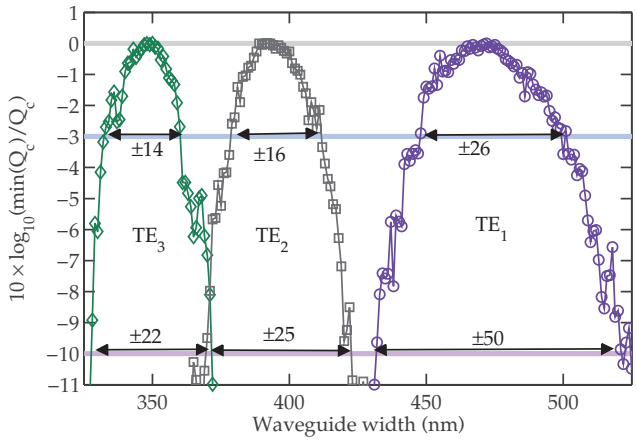

Fig. 5. The normalized $1/Q_c$ of the waveguide-cavity coupling in the pulley configuration as shown in Fig. 1(a). The three curves depict the coupling of the waveguides to each of the three lower radial order TE modes. Each curve is normalized to the best coupling for each mode (occuring at the perfect phase matching condition for each mode). The vertical axis is in dB scale. The requiring tolerance in Q_c imposes a certain accuracy requirement on the width of the fabricated waveguides; the required accuracy depends on the length of coupling (l), and the radial order chosen (TE_1, TE_2, or TE_3). When the coupling length is 30 μm and the coupling gap is 400 nm, the 3dB fabrication tolerance of the waveguide width (δW) is ± 26, ± 16 and ± 14 for the three first TE modes (TE_1-TE_3), respectively.

Another interesting feature is the width of each curve in Fig. 4 around its optimal point, which is an indicator of the tolerance of the optimal structure to the fabrication imperfection in the waveguide width W. It is clear from Fig. 4 that coupling to the lowest order resonance TE mode (i.e., TE_1) has better tolerance than that to the higher order modes. The tolerance of Q_c to

#119623 - $15.00 USD Received 6 Nov 2009; revised 15 Jan 2010; accepted 15 Jan 2010; published 19 Jan 2010

fabrication imperfections is shown in Fig. 5. In Fig. 5, the normalized Q_c^{-1} is plotted in the dB scale for the three lower radial order TE modes. Depending on the tolerance required for Q_c, the width of each curve identifies the acceptable error in the width of the fabricated waveguides (δW) when $g = 400$ nm. Based on Fig. 5, the acceptable fabrication error for the first three radial order modes (assuming only 3dB tolerance in Q) is $\delta W = \pm 26$ nm for TE_1, ± 16 nm for TE_2, and ± 14 nm for TE_3. These values, consideraing the high accuracy of the electron beam machine used, and also possibility of pre-fabrication corrections in the designs, is well within the achievable accuracy in our current fabrication facility.

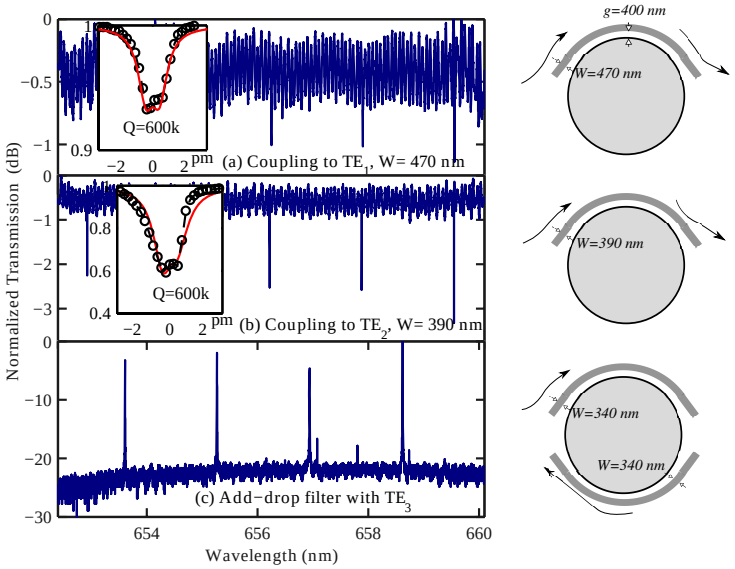

Fig. 6. The normalized transmission of a single-mode, curved waveguide coupled to a microdisk with radius $R = 20\,\mu$m in the pulley configuration as shown in Fig. 1(a). The coupling length is $l = 30\,\mu$m, and the coupling gap is 400 nm: (a) coupling to the first order microdisk TE mode with $W = 470$ nm; and (b) coupling to the second order microdisk TE mode with $W = 390$ nm. As the waveguide width is reduced, the effective index of the guided mode is reduced, thus higher order resonator modes are phase-matched to the waveguide. (c) The transmission spectrum of the drop port in an add-drop filter with both waveguides being 340 nm wide. Power is transferred to the drop port only when the third radial order TE mode of the microdisk is resonant.

To demonstrates the practicality of the optimal design criteria shown in Fig. 4, structures with three different waveguides widths (W=470, 390, and 340 nm) were fabricated in both single waveguide and add-drop configurations. The waveguides are all single mode for the desired range of wavelengths (652–660 nm). Figures 6(a) and 6(b) depict the normalized transmission for the single waveguides coupled to TE_1 and TE_2 with W of 470 nm and 390 nm, respectively. The coupling gap is 400 nm for all the fabricated structures. To identify the radial mode order in each case in Fig. 6, we compared the measured free spectral range (FSR) with the theoretically calculated FSRs of different radial mode orders. The resonant mode in the structure with $W =$ 470 nm [Fig. 6(a)] has the largest FSR=1.632 nm, and it corresponds to the TE_1 mode. Similarly the resonant dips in the transmission spectrum of the structure with W=390 nm [shown in Fig. 6(b)] correspond to an FSR of 1.658 nm and are attributed to the TE_2 mode.

Finally, Fig. 6(c) depicts the output of the drop waveguide when the through and the drop

#119623 - $15.00 USD Received 6 Nov 2009; revised 15 Jan 2010; accepted 15 Jan 2010; published 19 Jan 2010

waveguides are both chosen to be 340 nm wide. In such structures, power is transferred to the drop port only when the third order mode of the microdisk is in resonance. Thus, such an add-drop filter is practically single mode even though the microdisk—unlike a microring—is multimode.

Comparing Fig. 6 and Fig. 4 shows that for each waveguide width design, the waveguide mode couples better to the resonator mode for which stronger coupling (or smaller Q_c) exists. Figure 4(a) clearly shows that at $W = 470$ nm, 390 nm, and 340 nm, Q_c is the smallest for TE_1, TE_2, and TE_3, respectively. Thus the results shown in Fig. 6 confirm the finding in Fig. 4(a) about the optimal waveguide width (W) for each resonator mode.

4. Conclusion

In summary, we presented a detailed investigation of the properties of pulley coupled Si_3N_4 microdisk resonators on substrate at visible wavelengths. We showed that it is possible to fabricate these structures with larger coupling gaps taking advantage of the increased interaction length when the waveguide wraps around the resonator. Larger gaps make the reflow process possible to reduce the sidewall roughness of the microdisks and increase the quality factor of resonances. Moreover, the coupling along a pulley-shaped coupler is phase dependent and by choosing the proper width for the waveguide, single mode operation of the microdisk based devices (e.g. filters) is possible.

Acknowledgements

This work was supported by the Air Force Office of Scientific Research (AFOSR) through Dr. G. Pomrenke under contract No. FA9550–06–01–2003

#119623 - $15.00 USD Received 6 Nov 2009; revised 15 Jan 2010; accepted 15 Jan 2010; published 19 Jan 2010